Future changes in winter-time extratropical cyclones over South Africa from CORDEX-CORE simulations

Chinta, S., Schlosser, C. A., Gao, X. and Hodges, K. ORCID: https://orcid.org/0000-0003-0894-229X (2025) Future changes in winter-time extratropical cyclones over South Africa from CORDEX-CORE simulations. Earth's Future, 13 (1). e2024EF005289. ISSN 2328-4277 doi: https://doi.org/10.1029/2024EF005289 Available at https://centaur.reading.ac.uk/118515/

It is advisable to refer to the publisher's version if you intend to cite from the work. See [Guidance on citing](#).

www.reading.ac.uk/centaur

Future Changes in Winter-Time Extratropical Cyclones Over South Africa From CORDEX-CORE Simulations

Sandeep Chinta[1] , C. Adam Schlosser[1], Xiang Gao[1], and Kevin Hodges[2]

[1]Center for Sustainability Science and Strategy, Massachusetts Institute of Technology, Cambridge, MA, USA, [2]Department of Meteorology, National Centre of Atmospheric Science, University of Reading, Reading, UK

Abstract Extratropical cyclones (ETCs) significantly impact mid-latitude weather patterns and are crucial for understanding the societal implications of regional climate variability, climate change, and associated extreme weather. In this study, we examine the projected future changes in winter-time ETCs over South Africa (SA) using simulations from CORDEX-CORE Africa. We utilized three regional climate models, each driven by three different global climate models that simulate both the current climate and a future climate experiencing strong human-induced warming. From these, we assess changes in ETC frequency, track density, intensity, storm severity, and associated rainfall. The results indicate a significant reduction in the aggregate ETC frequency and track density, although track density is projected to increase prominently along the western coastal regions. Models show mixed trends in cyclone intensity projections, but overall results indicate weaker future cyclones, with reduced peak relative vorticity and increased minimum sea level pressure. Examining the Meteorological Storm Severity Index reveals notable regional variations in future storm severity. Average rainfall associated with ETCs is projected to decrease across SA, especially around Cape Town, highlighting a potential shift in the spatial distribution of rainfall with substantial consequences for water supply. We further investigated extreme ETCs (EETCs) and found that the trends for EETCs are generally similar to those for ETCs, with a notable decrease in frequency and regional variations in storm severity. These findings underscore the importance of developing targeted adaptation strategies to address the projected impacts of future ETCs on SA's climate and communities.

Plain Language Summary This study investigates how winter-time extratropical cyclones (ETCs) over South Africa might change in the future due to human-forced climate change. These storms are vital to the region as they bring heavy rain and strong winds, which can significantly impact local communities by affecting daily life, economic activities, human safety, and the environment. Using advanced climate model simulations under a high greenhouse gas scenario (RCP 8.5), we explored future changes in the frequency, intensity, and rainfall of these storms. Our findings suggest a potential decrease in the overall number of ETCs, with an increase in storm occurrences along the western coastal regions. The storms are projected to be generally weaker in terms of wind speed and may bring less rain overall. However, areas like Cape Town could experience more severe storms, leading to changes in rainfall patterns that could have substantial impacts on water resources, agriculture, and infrastructure. Additionally, we examined extreme ETCs and found similar trends, with a decrease in their number and varying changes in severity across different regions. Understanding these potential changes is crucial for developing strategies to minimize the adverse impacts on South Africa's environment and communities.

1. Introduction

Extratropical cyclones (ETCs) are key components of mid-latitude weather variability, significantly impacting regional climates with extreme winds and precipitation (Ulbrich et al., 2009). Additionally, ETCs are responsible for up to 90% of mid-latitude precipitation in storm tracks and up to 80% of extreme precipitation events, with the frequency and intensity of precipitation strongly influenced by ETCs (Catto et al., 2012; Hawcroft et al., 2012; McErlich et al., 2023). These weather systems can modulate the atmospheric general circulation, and the overall climate system (Fasullo & Trenberth, 2008; Peixoto & Oort, 1992) by transporting large quantities of heat, moisture, and momentum, thereby balancing the global energy and moisture budgets (Held & Soden, 2006; Trenberth & Stepaniak, 2004). ETCs are responsible for a majority of precipitation in mid-latitudes contributing to flooding (M. Hawcroft et al., 2018; Pfahl & Wernli, 2012). In the Southern Hemisphere (SH), the meteorology of the Southern Ocean is dominated by ETCs and their associated frontal systems, which play a significant role in

Writing – review & editing:
C. Adam Schlosser, Xiang Gao,
Kevin Hodges

the region's radiative balance and cloud field (Berry et al., 2011; Bodas-Salcedo et al., 2016; Utsumi et al., 2017). Given their significant role in the climate, it is crucial to understand how various characteristics of ETCs will change in the future, particularly in ETCs-prone regions, like South Africa.

ETCs in South Africa, particularly during winter months (June–July–August), cause extreme rainfall events and severe flooding and result in extensive damage to infrastructure, loss of property, and significant economic costs (Mahlobo et al., 2024). This is especially problematic in the Western Cape region, where thousands of people living in informal settlements are displaced annually due to the passage of ETCs (Lennard et al., 2013). In July and August 2001, a series of severe mid-latitude ETCs resulted in over R10 million (approximately USD 1.16 million at the 2001 exchange rate of 8.62) in damages in Cape Town, affecting around 8,000 homesteads (Lennard et al., 2013). Another event in August 2006 caused more than R500 million (approximately USD 73.74 million at the 2006 exchange rate of 6.78) worth of damage along the south coast of the country and resulted in nine deaths. The environmental impacts include soil erosion, surface denudation, and local slope slippages, potentially diverting watercourses and affecting local ecology and hydrology (Conradie et al., 2022; MacKellar et al., 2007). Standing water from flooding can increase the risk of waterborne diseases like cholera and lead to the release of agricultural and industrial pollutants into water sources, exacerbating health risks for local populations (Lennard et al., 2013).

Research to date has established a fundamental understanding of potential change to ETCs across the SH under human-forced climate warming. Consistent patterns across multiple generations of General Circulation Models (GCMs) have shown a robust poleward shift in the SH storm tracks (Bengtsson et al., 2009; Chang, 2017; Chang et al., 2012; Priestley & Catto, 2022a). This shift is attributed to forcings in the upper and lower troposphere and high-latitude heating at low levels, which push storm tracks poleward (Butler et al., 2010). Projections indicate a decrease in the total number of ETCs in SH, but an increase in associated precipitation (Chang et al., 2012; Geng & Sugi, 2003; Sinclair et al., 2020; Zappa et al., 2013). Specifically, cyclone intensity in the SH is expected to increase, with stronger seasonal variability (Chang, 2017; Chang et al., 2013; Lehmann et al., 2014). The magnitude and direction of these changes can vary depending on the model, variable, and region of interest (Catto et al., 2019; Ulbrich et al., 2009). Cyclone intensity, often defined by wind speed due to its socio-economic impacts, shows uncertain and regionally variable projections (Christensen et al., 2013). Studies assessing ETC intensity generally indicate an increase when using mean sea level pressure (MSLP) (Bengtsson et al., 2006; Mizuta et al., 2011), whereas those using vorticity show little change or reduction in intensity (Champion et al., 2011; Sinclair & Catto, 2023; Zappa et al., 2013). Despite extensive research on SH ETCs, studies focused on South African ETCs remain limited, hindering our understanding of local impacts and the implementation of adaptation strategies.

Projections of future changes in ETCs, especially at the regional scale, remain challenging due to the typical low resolution of current General Circulation Models (GCMs), such as those used in the Coupled Model Inter-comparison Project. This low resolution hampers the ability to accurately resolve important ETC processes (Ulbrich et al., 2009). High-resolution models enable the spatial detail necessary for capturing localized extreme events and improve the representation of topographical features and land-use patterns relevant to regional climate dynamics (Jacob et al., 2020). These models also offer increased accuracy in simulating extremes by capturing finer-scale atmospheric processes, resulting in better predictions of the intensity and frequency of such events (Forzieri et al., 2016; Giorgi, 2019; Murakami et al., 2012). Over the last few decades, regional climate models (RCMs) have been increasingly used as a tool for understanding regional-scale phenomena and assessing possible future climate change impacts. The need for high-resolution regional climate simulations has led to initiatives like the COordinated Regional Downscaling EXperiments (CORDEX)-COmmon Regional Experiment (CORE) Framework, which provides a 25 km high-resolution data set (Giorgi et al., 2021; Gutowski et al., 2016). CORDEX-CORE simulations cover different regional domains (including Africa) and have demonstrated a good performance in reproducing the general characteristics of ETCs and have been used to assess the response of ETC characteristics to global warming in different SH basins (Reboita et al., 2018, 2021a, 2021b). Although these studies explore South Africa among the SH basins, they analyze simulations from only one of the three available CORDEX-CORE Africa RCMs, limiting the understanding of the associated uncertainty. It is important to explore more RCMs to gain a comprehensive understanding of ETC behavior and projections, as different models can provide varying insights and enhance the robustness of the findings (Giorgi et al., 2009; Mearns et al., 2012).
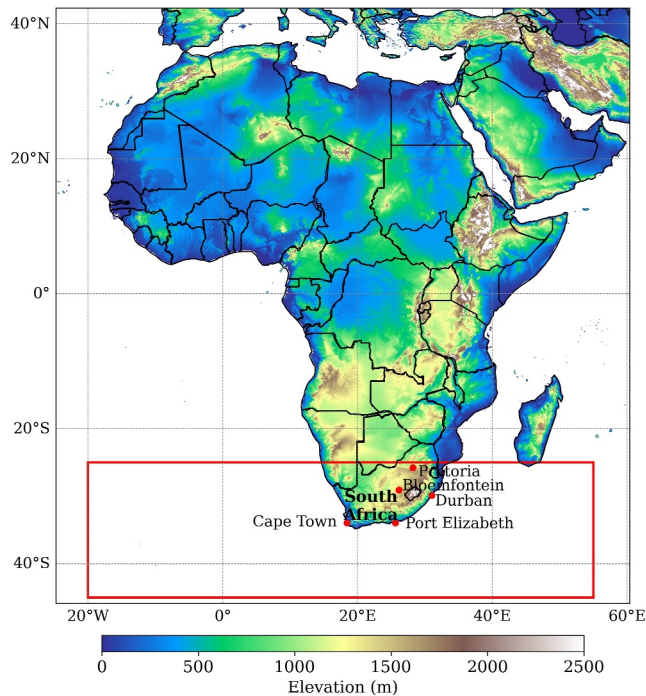
Figure 1. Topography of the CORDEX-CORE Africa domain. The region of interest for analyzing Extratropical cyclones is marked with a red boundary.

This study aims to investigate future changes in winter-time ETCs over South Africa using all available model simulations from the CORDEX-CORE Africa experiment. In addition to their role as drivers for RCMs, the three GCM model simulations were also directly analyzed in this study to provide a broader perspective on ETC characteristics and their changes at a coarser resolution. This dual approach allows for a more comprehensive understanding of ETC dynamics by leveraging both coarse-resolution GCM outputs and high-resolution regional insights. We focus on assessing how future climate will alter the intensity, frequency, track density, average track distance, duration, storm severity, and associated rainfall of winter-time ETCs and extreme ETCs (EETCs) in South Africa. This knowledge is essential for developing effective adaptation and mitigation strategies to alleviate local impacts.

2. Datasets and Methods

2.1. CORDEX-CORE Africa Simulations

We compile CORDEX-CORE Africa (AFR-22) simulations at ($0.22° \times 0.22°$ resolution) from three RCMs: the Climate Limited-area Modeling Community (CCLM) (Sørland et al., 2021), the RCM (RegCM) (Coppola et al., 2021; Giorgi et al., 2012, 2021), and the REgional MODel (REMO) (Jacob et al., 2012; Remedio et al., 2019). The CORDEX-CORE Africa domain is presented in Figure 1, along with five major cities in South Africa. Each RCM is driven by three global climate models (GCMs): the Max Planck Institute for Meteorology Earth System Model, low/medium resolution (MPI) (Giorgetta et al., 2013; Stevens et al., 2013), the Norwegian Earth System Model, version

1 (NorESM) (Bentsen et al., 2013; Iversen et al., 2013), and the Met Office Hadley Centre Global Environment Model, version 2 Earth System (HadGEM), as well as by ERA-Interim reanalysis data from the European Centre for Medium-Range Weather Forecasts (ERAI) (Dee et al., 2011). RCM historical simulations cover the periods 1950–2005, 1970–2005, and 1970–2005 for CCLM, RegCM, and REMO, respectively (https://cordex.org/experiment-guidelines/cordex-core/). Future simulations for all three models span from 2006 to 2100. For this study, only the RCP 8.5 scenario is analyzed. The reference period is defined as 1986–2005 (hereafter referred to as the historical period), while the end-of-century period is defined as 2080–2099 (hereafter referred to as the future period). For a more detailed overview of these RCMs and GCMs, refer to Safari et al. (2023) and Abel et al. (2024).

In total, we have nine simulations (three RCMs driven by three different GCMs) covering both historical and future periods. The ensemble mean of these nine simulations during the historical and future periods is referred to as RCM_Hist (9) and RCM_Fut (9), respectively. Similarly, we use GCM_Hist (3) and GCM_Fut (3) to represent the ensemble means of the three GCMs during the historical and future periods, respectively. The same abbreviation convention is adopted for the ensemble means of each RCM. For example, RegCM_Hist (3) [CCLM_Hist (3), REMO_Hist (3)] and RegCM_Fut (3) [CCLM_Fut (3), REMO_Fut (3)] refer to the ensemble means of the RegCM [CCLM, REMO] simulations driven by three GCMs for the historical and future periods. Additionally, a set of simulations where each of the three RCMs is driven by ERAI data from 1986 to 2005 will be used as a reference data set for evaluation (referred to as RCM_Eval (3) hereinafter).

2.2. Cyclone Identification and Tracking Algorithm

The method developed by Hodges (1994, 1995, 1999) is utilized for the objective identification and tracking of cyclones, following the approach described in Hoskins and Hodges (2002). This method is robust to the choice of input data (K. I. Hodges et al., 2011) and has been widely applied to both reanalyzes as well as global and RCMs (Bengtsson et al., 2004, 2006; Little et al., 2023; Priestley & Catto, 2022a; Tamarin & Kaspi, 2016; Torres-Alavez et al., 2021; Zappa et al., 2013). The algorithm employs 6-hourly relative vorticity at 850 hPa (ζ_{850}) as the tracking and identification variable, with a threshold value of ζ_{850} set at -1×10^{-5} s^{-1} for the SH. Relative vorticity is selected as the tracking and identification variable because it is less affected by the large-scale background state

than MSLP, is not an extrapolated field, and better captures smaller spatial scales (Hoskins & Hodges, 2002). Using vorticity also enables the identification of cyclones earlier in their life cycle, as a distinct vorticity feature may appear before a local pressure minimum develops.

Before identifying the cyclones, a pre-processing step is performed on ζ_{850} data to remove small-scale noise and large-scale planetary wave signals, focusing on synoptic-scale cyclones. For GCMs and ERAI data sets, ζ_{850} is spectrally truncated to T42 using spectral harmonic transform, with all wavenumbers less than or equal to 5 removed to eliminate planetary scales. This spectral filtering ensures the retention of synoptic scales and consistent resolution for all tracking, regardless of input data. For RCMs, a Discrete Cosine Transform (Denis et al., 2002) is applied to transform the data into frequency space, removing both small and large-scale noise equivalent to T42. The data is then transformed back to the original grid, retaining the original RCM resolution of 0.22° (~25 km) for tracking. Cyclones are initially identified by locating grid-point extrema that exceed the specified threshold, followed by refinement using B-spline interpolation and steepest ascent maximization. A track point, representing the location of a cyclone at a given time step, is then established. Cyclones are initialized into tracks by connecting consecutive track points using a nearest neighbor approach. These tracks are further refined by minimizing a cost function for track smoothness, subject to adaptive constraints for smoothness and displacement distance.

Tracks are filtered to retain those that persist for at least 48 hr and travel more than 1,000 km, focusing on long-lived, mobile storms. Since we are focusing on winter-time ETCs, we filter tracks for analysis that have at least one track point during the winter season. Although most of the RCM tracks are entirely within the region of interest (same as in Reboita et al. (2021b)) shown in Figure 1, a significant portion of track points for GCMs and ERAI are outside the study area. Therefore, only the track points within the interest region are retained for analysis. Mean sea level pressure (MSLP) values are assigned to tracks following Bengtsson et al. (2009), using the B-spline interpolation and minimization technique within a 5° radius from the cyclone center to identify the minimum MSLP value. Cyclone intensities are defined as the peak value of ζ_{850}. Extreme extratropical cyclones (EETCs) are characterized as those ETCs that exceed the 90th percentile of peak relative vorticity for that model. It's important to note that the 90th percentile is evaluated separately for each RCM, driven by different GCMs. We use the historical 90th percentile of peak relative vorticity for each model to identify the future EETCs for that model.

2.3. Meteorological Storm Severity Index (METSSI)

The Meteorological Storm Severity Index (METSSI) is a robust metric for quantifying storm severity, originally introduced by Klawa and Ulbrich (2003) as a loss proxy for European windstorms. Although initially applied to European windstorms, METSSI has significant potential for assessing storm severity in South Africa due to its robustness, adaptability, and strong association with extreme events. Its implementation contributes to a broader understanding of its applicability and effectiveness across diverse regions, allowing for the consistent assessment of ETCs globally. Derived from the Storm Severity Index, METSSI has been widely applied in numerous studies (Karremann, 2015; Karremann, Pinto, Von Bomhard, & Klawa, 2014; Leckebusch et al., 2007; Pinto et al., 2007, 2012). This metric utilizes 10 m wind speeds to assess storm severity, making it a valuable tool for evaluating the impacts of windstorms. METSSI captures the intensity and extent of extreme wind events over land areas by focusing on wind speeds exceeding the local 98th percentile, and isolating the metric for storm events over land areas. The calculation methodology, adopted from Little et al. (2023), involves considering wind speeds within a 5° radius of the track points, both 12 hr before and after the cyclone's passage (J. F. Roberts et al., 2014). The maximum wind speed values within this 24-hr period are used to create a "footprint" map, capturing the strongest winds associated with the cyclone (Catto et al., 2010; Priestley & Catto, 2022b). The METSSI at each grid point (i,j) is calculated to quantify the cumulative impact of all cyclones affecting that point, and it is given by the following equation:

$$\text{METSSI}_{ij} = \sum_c \left[\left(\frac{v_{ij}^{\max(c)}}{v_{ij}^{98}} - 1 \right)^3 . I\left(v_{ij}^{\max(c)}, v_{ij}^{98}\right) . L_{ij} \right]$$

$$I\left(v_{ij}^{\max(c)}, v_{ij}^{98}\right) = \begin{cases} 0 & \text{for } v_{ij}^{\max(c)} < v_{ij}^{98} \\ 1 & \text{for } v_{ij}^{\max (c)} \geq v_{ij}^{98} \end{cases}$$

$$L_{ij} = \begin{cases} 0 & \text{for} \quad \text{seas} \\ 1 & \text{for} \quad \text{land} \end{cases}$$

where $v_{ij}^{\max(c)}$ is the maximum wind speed at grid point (i,j) for a cyclone c within a 24 hr period (12 hr before and after the cyclone's passage). v_{ij}^{98} is the local 98th percentile of 6-hourly wind speeds at grid point (i,j), based on climatology (not cyclone-specific). This value is used as the damage threshold. The indicator function $I\left(v_{ij}^{\max(c)}, v_{ij}^{98}\right)$ ensures that only wind speeds exceeding the 98th percentile contribute to the METSSI. L_{ij} is a land-sea mask that ensures that only land grid points are considered in the METSSI calculation.

To ensure lower wind speeds do not influence the loss metrics, all local 98th percentile wind speeds below 9 m/s were adjusted to this threshold (Karremann, Pinto, Von Bomhard, & Klawa, 2014). For METSSI calculations in the future simulation periods, we consider two cases based on Little et al. (2023): the No Adaptation (NAD) case and the Adaptation (AD) case. In the NAD case, historical v^{98} values are used for evaluating future METSSI, assuming no changes in building resilience or exposure. In the AD case, the historical v^{98} values are adjusted upwards to the future values at a grid point when the future v^{98} is greater than the historical value. If the future v^{98} is lower, the historical value is retained at that grid point, assuming that buildings and exposure do not de-adapt.

3. Results and Discussion

3.1. Frequency and Track Density

Figure 2a shows the average frequency of ETCs per season across different experiments and scenarios. The ERAI, serving as a reference, shows an average frequency of 64.0 ETCs per season. Both evaluation simulations (RCM_Eval, driven by ERAI) and historical GCM simulations (GCM_Hist) suggest some underestimation, with lower average frequencies of 53.5 and 61.3 ETCs per season, respectively. Historical RCM simulations (RCM_Hist, driven by GCM_Hist) exhibit a comparable average frequency of 60.9 ETCs per season, similar to GCM_Hist. Future RCM simulations (RCM_Fut) also show a comparable average frequency to GCM_Fut, indicating consistency between the frameworks in projecting future trends. Although the frequency of ETCs in RCMs is similar to that in GCMs for historical and future scenarios, the frequency of ETCs in the evaluation simulations (RCM_Eval) is noticeably lower compared to ERAI. It is important to note that the retention of ERAI and GCM tracks within the region of interest may result in these tracks being at different stages of their lifecycle compared to RCM tracks, whose entire lifecycle typically occurs within the region of interest. Such differences could influence direct comparison in track density and frequency between ERAI, GCM, and RCM simulations. We therefore focus on within-framework comparisons (e.g., RCM_Hist vs. RCM_Fut and GCM_Hist vs. GCM_Fut) to ensure consistency in track lifecycle representation. Future projections reveal an overall decrease in ETC frequency. GCM (GCM_Fut) and RCM (RCM_Fut) simulations indicate an average of 56 ETCs per season, corresponding to approximately an 8.6% and 7.2% decrease, respectively, compared to their historical counterparts. These changes are statistically significant, with a p-value less than 0.05 using the t-test. Figure S1 in Supporting Information S1 shows detailed breakdowns for individual GCMs and RCMs, all of which consistently demonstrate a robust decreasing trend in future ETC frequencies compared to their historical counterparts.

Track density, defined as the number of tracks passing through each grid point, reveals significant changes between future and historical simulations for GCMs (Figure 2b). The data indicates an overall decrease in track density, particularly in the southern and eastern parts of the region of interest, suggesting a spatial shift in ETC tracks in future projections. This pattern is consistent with Figure 2a, which shows a decrease in ETC frequencies in future projections compared to historical averages. However, a notable increase in track density is observed along the west coast of South Africa, and, in general, the track density over South African land is projected to be higher in the future compared to the historical period. The track density difference patterns from RCMs (Figure 2c) mirror these findings, with a decrease in track density in the southern and eastern parts of the region and an increase along the west coast of South African land. Further detailed breakdowns of track densities for individual GCMs (Figure S2 in Supporting Information S1) and RCMs (Figure S3 in Supporting Information S1) also show similar patterns. This consistency across both GCM and RCM simulations underscores a shift in the spatial distribution of ETC tracks.
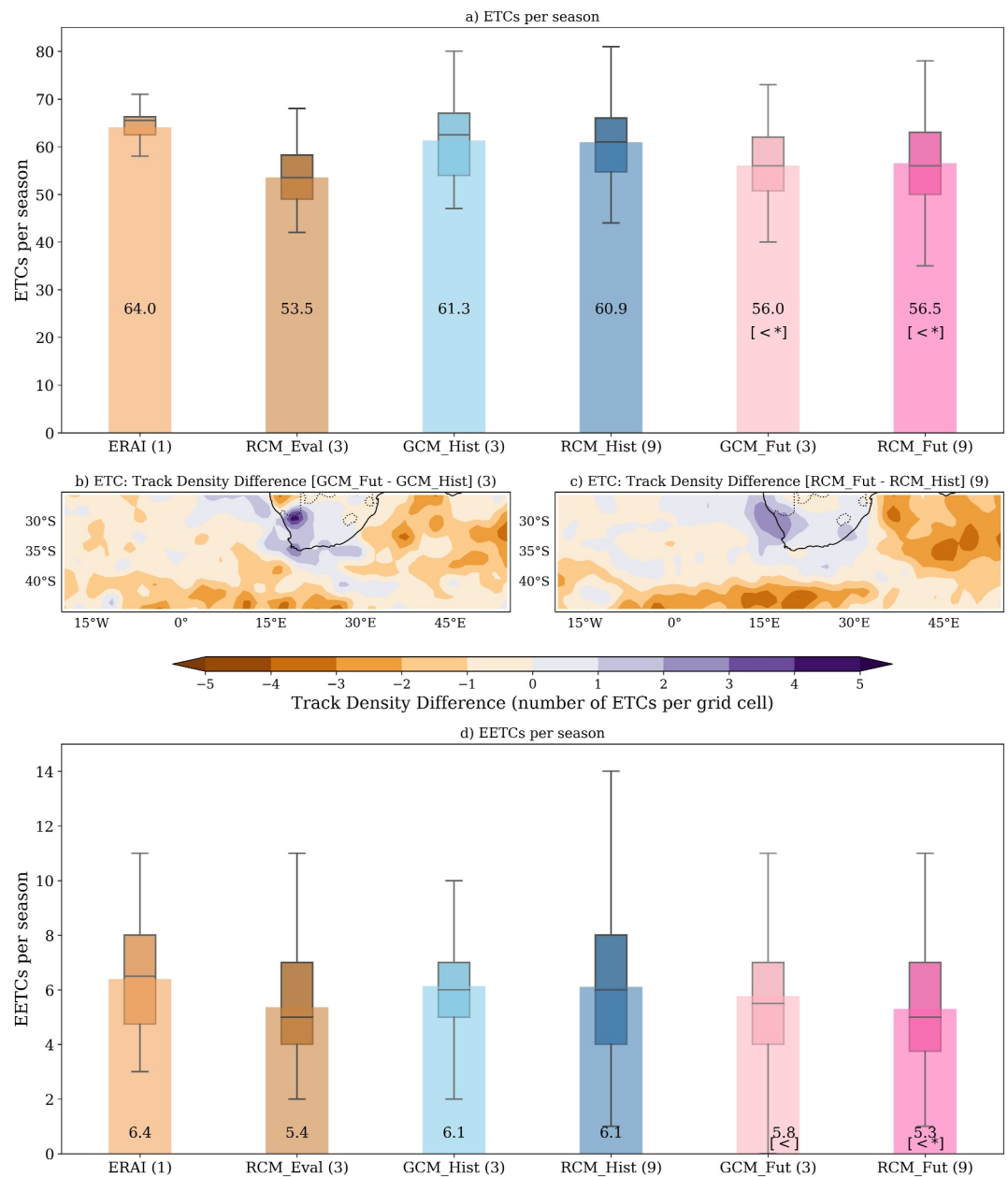
Figure 2. (a) Bar plots showing the average frequency of Extratropical cyclones (ETCs) per season across different experiments and scenarios. The numbers on the bars show the average frequency value for that experiment. The experiments include ERAI (1), RCM_Eval (3), GCM_Hist (3), RCM_Hist (9), GCM_Fut (3), and RCM_Fut (9). The numbers in brackets besides experiment names represent the number of model simulations averaged to obtain the ensemble for that experiment. The box plots represent the variability in frequency across winter seasons over the years. The symbol [<] indicates a future sign compared to historical averages, and [*] indicates the statistical significance of the change. (b) Track Density Difference [GCM_Fut - GCM_Hist] (3) shows the difference in ETC track density between future (GCM_Fut) and historical (GCM_Hist) simulations using three model simulations. (c) Track Density Difference [RCM_Fut—RCM_Hist] (9) shows the difference in ETC track density between future (RCM_Fut) and historical (RCM_Hist) simulations using nine model simulations. (d) Bar plots showing the average frequency of EETCs per season across different experiments and scenarios.

Figure 2d presents the frequency of EETCs per season across various experiments and scenarios. The ERAI experiment shows an average of 6.4 EETCs per season, while evaluation simulations (RCM_Eval) driven by ERAI show a lower average of 5.4 EETCs. Historical GCM simulations (GCM_Hist) have an average of 6.1 EETCs, slightly lower than ERAI, with corresponding RCM simulations (RCM_Hist) showing a comparable 6.1

EETCs per season. These values represent about 10% of the corresponding ETC frequencies, consistent with established EETC definitions. Future projections indicate a decrease in EETC frequency, with GCM simulations (GCM_Fut) averaging 5.8 EETCs per season, suggesting a 5% decrease compared to GCM_Hist. Similarly, RCM projections (RCM_Fut) indicate a 13% decrease, with an average of 5.3 EETCs per season. The changes in RCMs are statistically significant, unlike those in GCMs. Despite an average of around 6 EETCs per season, variability remains high, ranging from 0 to 14, highlighting significant inter-seasonal variability. Figure S4 in Supporting Information S1 provides detailed breakdowns for individual GCMs and RCMs, showing a generally decreasing trend in future EETC frequencies, with RCMs consistently aligning with the overall trends. The track density difference was not evaluated for EETCs as the number of EETCs was substantially smaller compared to ETCs, making it insufficient for a meaningful comparison. We analyzed the counts of EETCs within specific sub-domains identified based on regions of increase (20–35°S, 10–25°E) and decrease (37–45°S, 10–25°E) in ETC track density. This analysis revealed that EETCs also exhibit a spatial pattern similar to ETCs in the RCMs, with increases in the northern subdomain and decreases in the southern subdomain, consistent with broader regional trends.

3.2. Intensity: Peak Relative Vorticity and Minimum Mean Sea Level Pressure

Figure 3a presents the box plots of peak relative vorticity for all ETCs and EETCs across various experiments and scenarios. The higher peak relative vorticity of EETCs reflects their classification as extreme events and underscores their greater potential for severe impacts compared to ETCs. Both historical and future simulations demonstrate that RCMs generally exhibit higher average peak relative vorticity values for both ETCs and EETCs compared to GCMs. GCM simulations (GCM_Fut) project similar average peak relative vorticity values for ETCs and an increase for EETCs compared to the respective GCM_Hist values, with both changes not statistically significant. In contrast, RCM projections (RCM_Fut) indicate a decrease in average peak relative vorticity values for ETCs, whereas the average values for EETCs remain similar compared to the respective RCM_Hist values, with the change for ETCs being statistically significant. Although there is a general trend of decreasing future peak relative vorticity values for RCMs, the most intense ETCs (outliers) in both GCM and RCM simulations exhibit higher peak relative vorticity values in the future than the maximum peak relative vorticity values observed in their respective historical models. This suggests that the most extreme ETCs are likely to intensify further in the future, which could result in greater impacts, such as increased wind speeds, heavier precipitation, and potentially more severe socio-economic consequences. Individual GCMs show inconsistent responses, with NorESM displaying a unique trend of decreasing peak relative vorticity for ETCs and EETCs, unlike the other models (Figure S5a in Supporting Information S1), while RCMs generally indicate a consistent decrease in peak relative vorticity for ETCs but show mixed trends for EETCs (Figure S5b in Supporting Information S1). Overall, while there is some divergence in average peak relative vorticity projections between GCMs and RCMs, both modeling approaches consistently highlight the potential for the most extreme ETCs to intensify in the future, underscoring their likely greater impacts on weather extremes and associated risks.

Figure 3b presents the box plots of minimum MSLP for all ETCs and EETCs across various experiments and scenarios. EETCs consistently exhibit lower minimum MSLP values, reflecting their higher intensity compared to ETCs. Future projections indicate a clear trend of increasing MSLP values, suggesting a weakening of cyclones. Both GCM and RCM future simulations (GCM_Fut and RCM_Fut) show an increase in minimum MSLP values, with statistically significant changes. This consistent pattern across GCM and RCM simulations suggests a future decrease in cyclone intensity, as indicated by higher minimum MSLP values. Unlike the slightly mixed trends observed in peak relative vorticity, the MSLP results show a more uniform signal of weakening cyclones for the future simulations. Individual GCMs (MPI, HadGEM, and NorESM; Figure S6a in Supporting Information S1) show a consistent increase in future ETC minimum MSLP, with HadGEM and NorESM also indicating an increase in EETCs. The RCMs (RegCM and CCLM; Figure S6b in Supporting Information S1) exhibit a mix of trends, with both models showing an increase in ETC minimum MSLP and RegCM also showing an increase in EETCs. These results collectively suggest a potential future decrease in cyclone intensity as indicated by higher minimum MSLP values across both GCMs and RCMs.

3.3. Average Track Duration and Distance

Figure 4a presents the bar and box plots of average track duration per season for all ETCs and EETCs across various experiments and scenarios. Track duration is used as an indicator of the longevity of cyclones, with longer
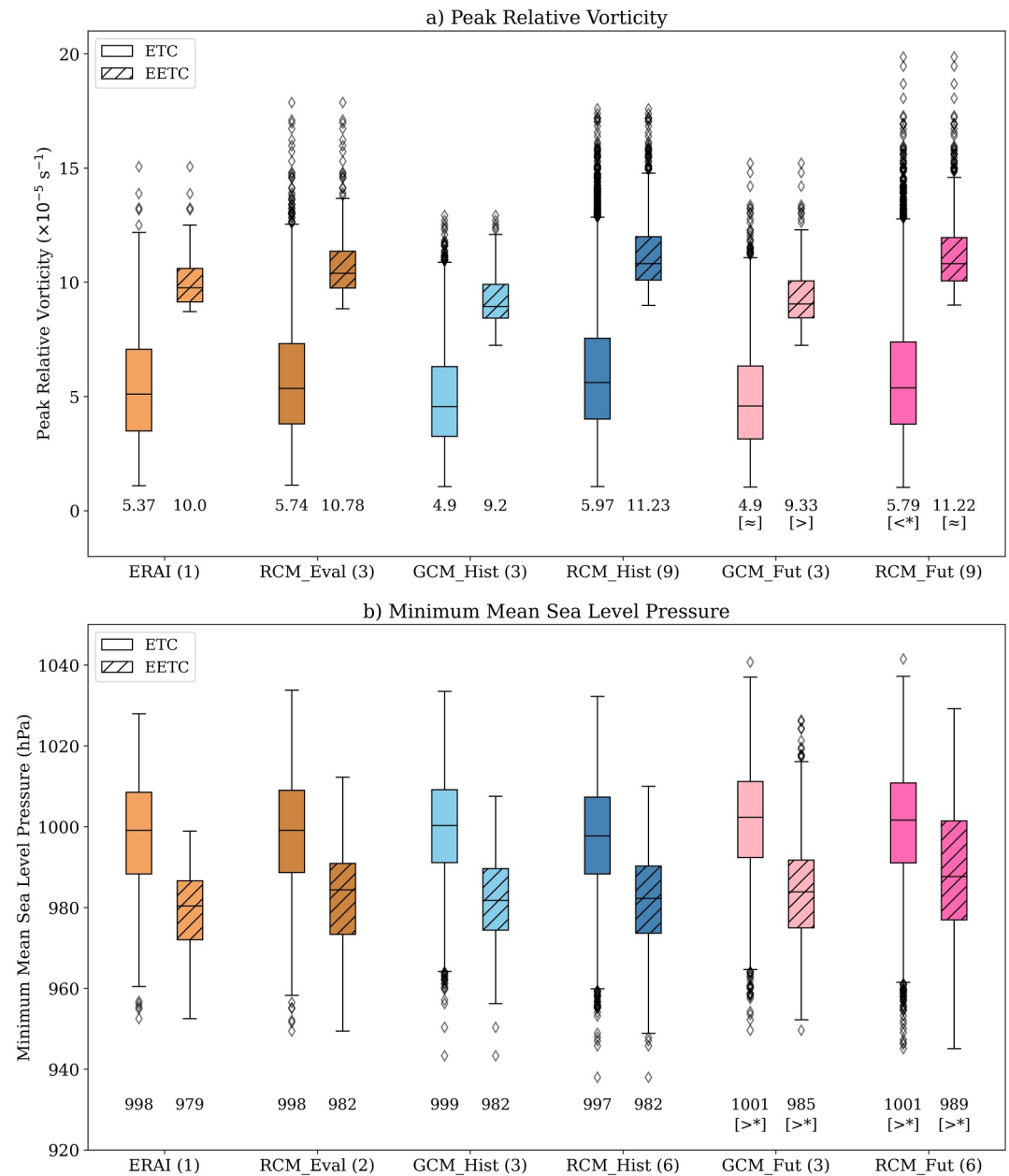
Figure 3. Box plots of (a) peak relative vorticity and (b) minimum mean sea level pressure (MSLP) for all extratropical cyclones and extreme extratropical cyclones across various experiments and scenarios. The numbers below the box plots show the average value for that experiment. All relative vorticity values are given in units of 10^{-5} s^{-1}. The minimum MSLP values are shown in hPa. The experiments include ERAI (1), RCM_Eval (3), GCM_Hist (3), RCM_Hist (9), GCM_Fut (3), and RCM_Fut (9). Symbols [<], [>], and [≈] indicate future changes compared to historical values, while [*] indicates statistical significance of the change. Note that REgional MOdel sea level pressure outputs are not available and are excluded from the MSLP analysis in panel (b).

durations suggesting a more prolonged impact. EETCs consistently exhibit longer average track durations than ETCs across all experiments and scenarios, underscoring the more prolonged impact of these more intense cyclones. RCM tracks are longer than GCM and ERAI tracks across all experiments as the track points for GCMs and ERAI outside the region of interest are trimmed. It is important to note that although the ERAI average track duration is 38.3 hr, which is less than the 48-hr threshold used to filter cyclones earlier, this is due to the trimming of ERAI track points outside the region of interest. Future projections show a clear pattern of decreasing track duration values compared to the historical values, with both GCM and RCM projections indicating reductions in
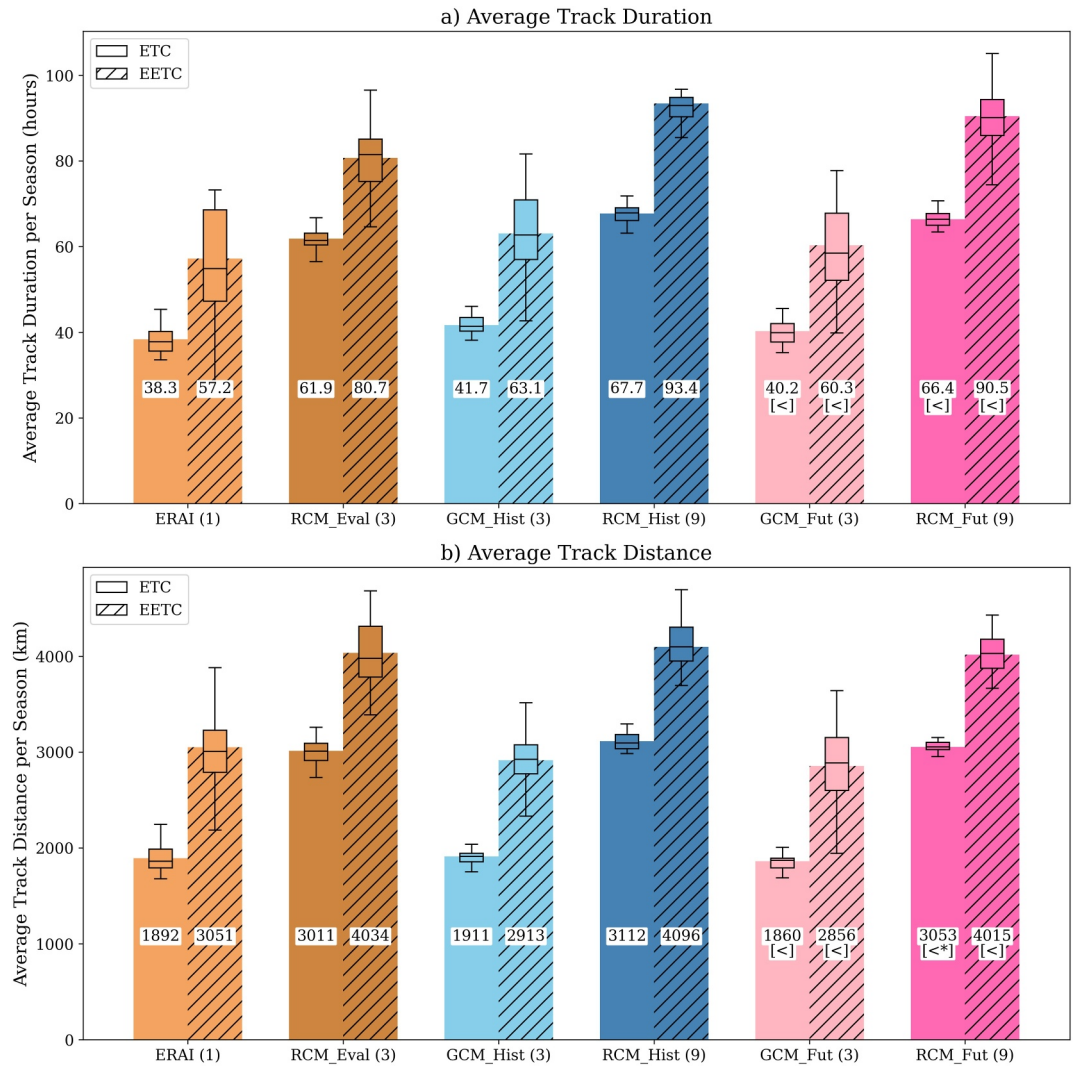
Figure 4. Bar and box plots showing (a) average track duration and (b) average track distance per season for Extratropical cyclones and EETCs across various experiments and scenarios. The bar plots represent the average values, while the box plots show the variability. The numbers on the bars show the overall average value for that experiment. The experiments include ERAI (1), RCM_Eval (3), GCM_Hist (3), RCM_Hist (9), GCM_Fut (3), and RCM_Fut (9). The numbers in brackets represent the number of model simulations averaged to obtain the ensemble for that experiment. The box plots represent the variability in frequency across seasons. The symbol [<] indicates a future sign compared to historical averages, and [∗] indicates the statistical significance of the change.

average track durations for both ETCs and EETCs. However, these decreases are not statistically significant. Additionally, the variability in average EETC track durations is higher compared to ETCs, indicating a wider range of possible durations for the more intense cyclones. Both GCMs (Figure S7a in Supporting Information S1) and RCMs (Figure S7b in Supporting Information S1) consistently show a clear decreasing trend in the average track duration of future ETCs and EETCs. This trend is observed across all models, reinforcing the overall finding that future cyclones are likely to have shorter track durations. These individual model results align with the general pattern of shorter cyclone tracks in future scenarios.

Figure 4b presents the bar and box plots of average track distance per season for all ETCs and EETCs across various experiments and scenarios. Track distance is used as an indicator of the spatial extent of cyclones, with longer distances suggesting a broader impact. EETCs consistently exhibit longer track distances than ETCs across all experiments and scenarios, underscoring the broader impact of these more intense cyclones. RCMs exhibit higher average track distances than GCMs, both historically and in future scenarios. Future projections indicate a

general trend of decreasing track distances for both ETCs and EETCs compared to historical values. While the decreases in track distances are more pronounced in RCM projections (RCM_Fut) and statistically significant for ETCs, the trend persists across all models. Further breakdowns for individual GCMs (Figure S8a in Supporting Information S1) and RCMs (Figure S8b in Supporting Information S1) show a general decreasing trend in future ETC and EETC average track distances. Notably, all models, except for a slight increase in EETCs by NorESM, indicate a decline in both ETC and EETC track distances. These individual model results highlight the general decreasing trend in average track distance across most models, reinforcing the overall finding that future cyclones may cover shorter distances. These findings are consistent with the conclusions drawn from the analysis of average track duration. Both metrics show a general decrease in future projections compared to historical values, although most changes are not statistically significant. This parallel in both track duration and distance reinforces the understanding that future cyclones may have shorter durations and cover shorter distances, potentially indicating a reduction in their overall spatial and temporal impact.

3.4. Meteorological Storm Severity Index

The METSSI is a crucial metric for quantifying storm severity, focusing on extreme wind events. One essential parameter in calculating METSSI is the 98th percentile of 10 m wind speeds (v^{98}), a threshold for identifying significant wind events. Since some GCMs do not provide 10 m wind speed data at a 6-hourly frequency (which matches the track points' frequency), this analysis is restricted to RCMs. Figure 5a shows the ensemble average change in v^{98} between future and historical periods for RCMs. The ensemble average reveals a significant increase in v^{98} over the interior regions of South Africa, particularly in the central region of South Africa, where the values exceed 0.45 m/s. This suggests a potential increase in the frequency or intensity of extreme wind events in these areas. Conversely, the coastal regions, especially along the southern and southeastern coasts near Cape Town, Durban, and Port Elizabeth, show a decrease in v^{98}, with values dropping below -0.15 m/s. Individual RCM results show different spatial patterns (Figure S9 in Supporting Information S1), reflecting the inherent variability and uncertainty in regional climate projections. However, the overall patterns of change trends observed in the ensemble average are consistent across most individual RCM results. RegCM and CCLM show substantial increases in v^{98} in the central regions and decreases along the coast, while REMO exhibits a more moderate increase in the central regions and a more prominent decrease in the regions slightly inland from the coast.

Figure 5b displays the difference in the METSSI for ETCs between a future scenario under the no adaptation (NAD) case and the historical period. The spatial distribution indicates regions with both increases and decreases in METSSI. Notably, the northwestern, central, and southeastern parts of South Africa exhibit a prominent decrease in METSSI. In contrast, the northern, some eastern parts, and the southern coast of South Africa, particularly around the Cape Town area, show an increase in METSSI. The track density difference (Figure 2b) for ETCs between the future and historical periods provides crucial insight into the changes in METSSI. Regions with increased (or decreased) track density often correlate with areas of increased (or decreased) METSSI in Figure 5b, such as northern and southern South Africa, suggesting that a greater number of cyclone tracks in the future leads to more frequent or severe wind events. However, there are areas, particularly in central to southeastern South Africa, where track density is projected to increase in the future, yet METSSI decreases. This apparent contradiction is likely due to changes in the intensity of wind speeds relative to the 98th percentile threshold. If the maximum wind speeds ($v_{ij}^{\max\,(c)}$) associated with future ETCs in these regions are not significantly higher than the historical v_{ij}^{98}, the indicator function $I\left(v_{ij}^{\max(c)}, v_{ij}^{98}\right)$ would limit their contribution to the METSSI. Thus, while more tracks may occur, their reduced intensity relative to the damage threshold results in a lower overall METSSI. Additionally, changes in the characteristics of ETCs, such as their structure, size, or the distribution of wind speeds within the storms, could lead to different impacts on METSSI. For example, future ETCs may have broader but less intense wind fields, with the wind energy spanning a larger area but not exceeding the critical thresholds to significantly impact METSSI. Overall, these findings underscore the complexity of projecting future storm impacts and highlight the importance of considering multiple factors in assessing storm severity. Results for each of the RCMs (Figure S10 in Supporting Information S1) suggest substantial variability among the models. While there is a general indication of decreasing storm severity in the central regions and increasing severity in the north and along the southern coast. Among the models, RegCM4 appears to drive the ensemble differences more significantly due to its widespread and intense anomalies, particularly over central and
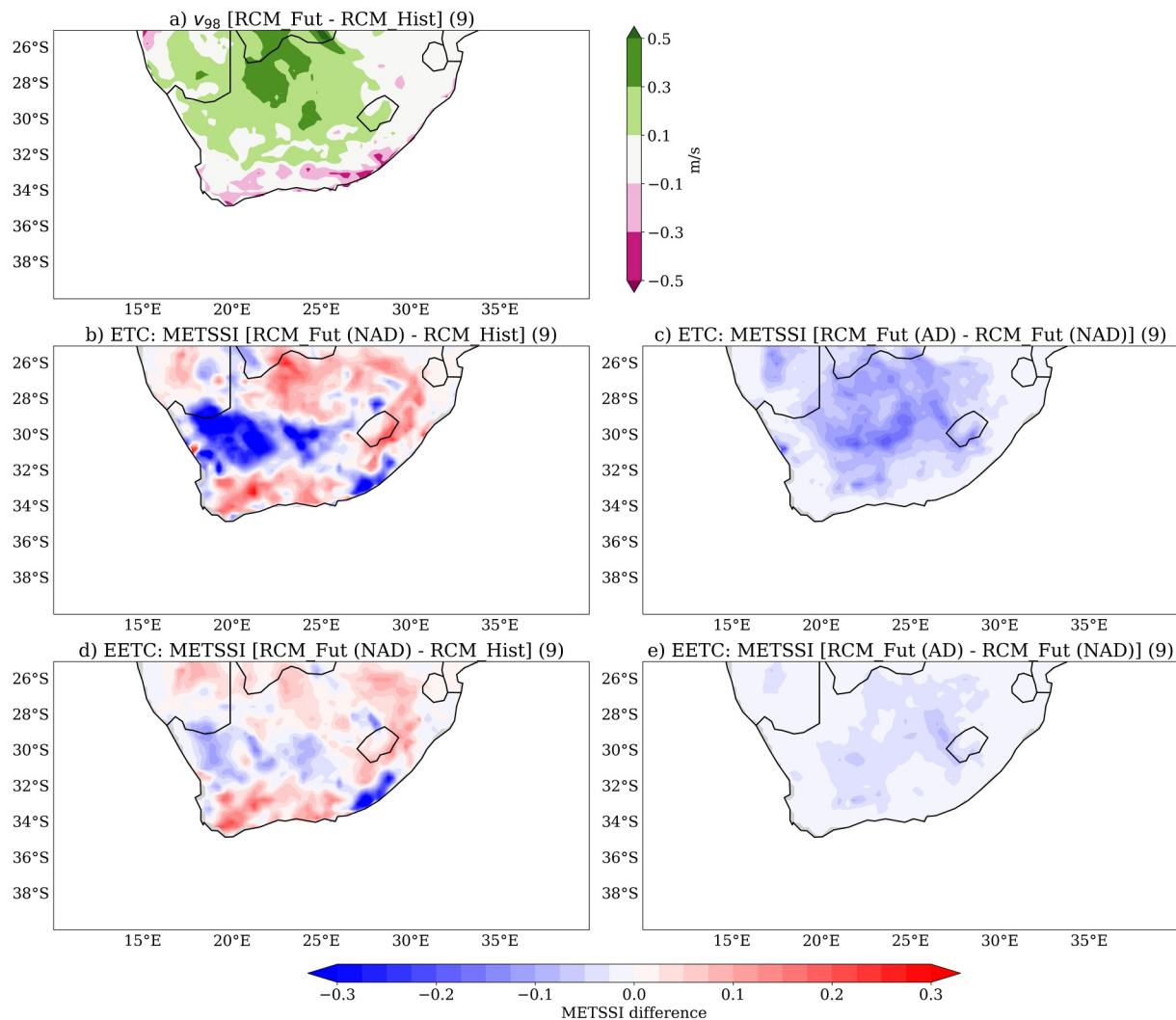
Figure 5. Spatial distribution plots over South Africa for the regional climate model (RCM) ensemble average: (a) difference in the 98th percentile of 10 m wind speeds (v^{98}) between future and historical period. (b) difference in Meteorological Storm Severity Index (METSSI) for Extratropical cyclones (ETCs) between future under the no adaptation (NAD) case and historical period. (c) same as (b) but for EETCs. (d) difference in METSSI for ETCs between future adaptation (AD) case and future no adaptation (NAD) case for the RCM ensemble. (e) same as (d) but for EETCs.

northern South Africa. These broader and more pronounced changes in RegCM4 contribute substantially to the overall trends, in contrast to the localized high-intensity anomalies in REMO and the relatively muted changes in CCLM. The magnitude and extent of these changes vary significantly across models.

In the adaptation (AD) case, the historical v^{98} values are updated with future values wherever the future v^{98} is higher, reflecting a scenario where resilience to extreme wind events improves over time. These adaptation measures could include strengthening building codes, retrofitting existing structures, and implementing urban planning strategies to better withstand the impacts of more severe ETCs. The spatial distribution shows that central parts of South Africa generally exhibit a decrease in METSSI in the AD scenario relative to the NAD scenario measures (Figure 5c). These changes in METSSI are closely related to the changes in v^{98} values (Figure 5a). Regions where future v^{98} values are higher typically show a reduction in METSSI difference, indicating that increased thresholds reduce the severity index. The adaptation measures could reduce the potential impact of ETCs in these regions, particularly those regions where METSSI is projected in increase in the future such as the northern parts of South Africa. However, the southern regions where METSSI is projected to increase in the future, adaptation measures show no significant impact. This suggests that, apart from adaptation, more proactive and targeted measures are needed to address the increasing METSSI in these regions effectively. A
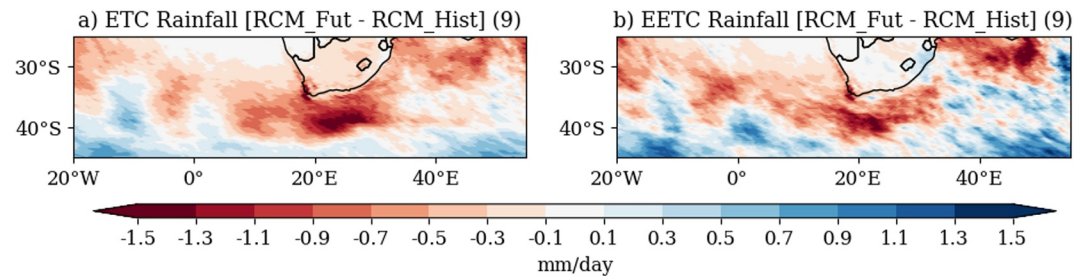
Figure 6. Spatial patterns over South Africa for the difference in average rainfall associated with (a) extratropical cyclones and (b) extreme extratropical cyclones between future and historical periods for the regional climate model ensemble.

detailed breakdown across RCMs (Figure S11 in Supporting Information S1) shows that RegCM displays large decreases in METSSI across significant areas, indicating strong adaptation benefits. In contrast CCLM and REMO show more moderate decreases.

The spatial distribution of EETCs strongly resembles that of ETCs (Figure 5d). The northern and southern coastal regions, particularly around Cape Town, exhibit an increase in METSSI, while central to southeastern South Africa shows a decrease in METSSI. Since EETCs are lesser in number, the decreases in METSSI are not as pronounced as those observed for ETCs, where more regions experienced a significant reduction. Despite some variability among different RCMs (Figure S12 in Supporting Information S1), there are signals indicating decreasing storm severity in the central to southeastern regions and increasing severity in the northern and southern coastal areas, including Cape Town. Similar to ETCs, the adaptation measures generally result in a decrease in METSSI in most parts of South Africa, indicating that these measures could effectively reduce the severity of EETCs in these regions (Figure 5e). Results from individual RCMs (Figure S13 in Supporting Information S1) reveal that RegCM exhibits substantial decreases in METSSI across extensive areas, while CCLM and REMO show more moderate decreases.

3.5. Rainfall

Figure 6a illustrates the projected changes in ETC-associated average rainfall for the future compared to the historical period. We consider cyclone-associated rainfall as the rainfall occurring over the region of interest during the cyclone's track duration. Since some of the GCMs considered do not provide rainfall data at a 6-hourly frequency (which matches the track points' frequency), this analysis is restricted to RCMs. A prominent decrease in rainfall over South Africa is particularly evident in the southern regions around Cape Town. Moving toward the central parts of South Africa, the changes are less pronounced, with minor variations indicating slight decreases. Additionally, the eastern coast of South Africa also exhibits a reduction in rainfall. Offshore regions to the southwest show a heterogeneous pattern, with both slight increases and decreases in rainfall. Overall, the figure suggests a general trend of decreased ETC-associated average rainfall over southern Africa, with notable increases in the South Indian Ocean and South Atlantic Ocean, indicating a shift in the spatial distribution of simulated rainfall associated with ETCs in the future climate scenario. A detailed breakdown across RCMs (Figure S14 in Supporting Information S1) indicates that REMO is contributing more significantly to the overall differences compared to other models. REgional MOdel shows stronger anomalies, particularly over the southern regions of South Africa. These anomalies are more intense compared to those from RegCM4 and CCLM. While the general trends across models are consistent, REMO amplifies the observed changes, especially with larger reductions in rainfall over southern regions of South Africa around Cape Town. Despite some minor variations and heterogeneous patterns in offshore areas, the general trend points toward a drier future for South Africa with respect to ETC-associated rainfall.

In comparison to the general ETC rainfall patterns, EETC rainfall changes (Figure 6b) display a more varied pattern over South Africa. While there is still a marked reduction in rainfall over the southern regions, including Cape Town, there are also notable increases in EETC-associated rainfall in central and eastern parts of South Africa. Offshore regions display similar heterogeneous patterns, with both increases and decreases. Additionally, the increases in EETC-associated rainfall are more prominent over the South Indian Ocean and South Atlantic Ocean. A detailed breakdown across RCMs (Figure S15 in Supporting Information S1) reveals a variety of

patterns, including decreases in EETC-associated rainfall over the southern and western regions of South Africa, as well as increases across eastern South Africa. This comparative analysis across RCMs highlights the variability and complexity in the projected changes of EETC-associated rainfall, with both increases and decreases evident in different regions.

3.6. Discussion

In our analysis, we employed a multi-model ensemble approach, utilizing nine simulations derived from three different RCMs driven by three distinct GCMs. This ensemble-based approach is important in capturing a range of possible future outcomes, as individual RCMs can exhibit varying responses to the same climate forcings. To complement this, we also incorporated analysis from the three driving GCM simulations to provide a broader perspective and contextualize the RCM findings. By integrating these diverse results, we achieve a more balanced and comprehensive picture of future climate impacts on ETCs over South Africa. This ensemble approach not only enhances the robustness of our findings but also provides a more reliable basis for developing adaptation strategies, as it accounts for the inherent uncertainties across different models.

In this study, we observe that ERAI generates a higher number of storms compared to GCMs, primarily due to its finer spatial resolution, which allows it to better capture small-scale atmospheric dynamics (Booth et al., 2018; Iles et al., 2020). ERAI also benefits from more sophisticated convective parameterization schemes, resulting in more realistic storm structures than those simulated by the simpler schemes used in GCMs (Booth et al., 2018). Furthermore, GCMs often simulate weaker surface winds, which are crucial for the accurate formation of ETCs, thereby leading to fewer detected storms (Booth et al., 2018). Despite the higher resolution of RCMs like those in the CORDEX-CORE framework, the number of detected ETCs is often similar to that in GCMs due to several limiting factors. One key factor is the restricted domain of RCMs, which are typically focused on specific regions and may miss cyclones that form or travel outside their boundaries. For instance, the CORDEX-CORE Africa domain extends to approximately 45°S, potentially excluding cyclones forming further south. Additionally, RCMs are constrained by the boundary conditions provided by their parent GCMs, which can limit their ability to fully exploit their higher resolution and accurately simulate storm development and intensification near the domain edges (Dowdy et al., 2013; Elguindi et al., 2014). These boundary effects and the partial capture of storm tracks can result in cyclone counts that are similar to those in GCMs.

Future climate projections indicate a reduction in the number of ETCs over South Africa. Notably, Reboita et al. (2021b) used an automatic cyclone detection and tracking method (CDTM) developed by Lionello et al. (2002) and Reale and Lionello (2013) to identify ETC tracks over South Africa for the RegCM model. Their findings also projected a reduction in track frequency over South Africa in the future. A primary driver is the expected decrease in baroclinicity, the temperature gradient between the equator and the poles, which is crucial for cyclogenesis. As this gradient weakens, the potential for cyclone formation diminishes. Additionally, climate models project a poleward shift and potential weakening of the SH jet streams, which play a critical role in the development and intensification of ETCs. This shift further reduces the frequency of ETCs in mid-latitudes over South Africa while potentially increasing activity closer to Antarctica (Chang et al., 2012; Priestley & Catto, 2022a). Moreover, increased atmospheric stability due to higher temperatures suppresses the vertical motions necessary for storm development, contributing to an overall reduction in ETC activity (Dowdy et al., 2013; Parsons et al., 2016). While a general reduction in ETC tracks is expected due to a poleward shift in storm tracks, the west coast of South Africa is projected to experience an increase in storm activity. This can be attributed to rising atmospheric moisture and enhanced localized increases in upper-tropospheric baroclinicity. The meandering jet streams associated with this shift can lead to prolonged and intensified storm activity in specific regions (Moon et al., 2022; Palipane et al., 2017).

Track intensity projections for ETCs show notable differences between GCMs and RCMs in terms of future changes in peak relative vorticity. RCMs consistently show higher absolute values of peak relative vorticity compared to GCMs across both historical and future simulations. RCMs generally project a significant reduction in future peak relative vorticity, whereas GCMs indicate similar values in future for ETCs. For EETCs, GCMs project an increase in future peak relative vorticity, whereas RCMs suggest similar values across historical and future simulations. This discrepancy in future trends might be due to the higher resolution of RCMs, which allows them to capture more localized and intense atmospheric phenomena that GCMs, with their coarser resolution, may smooth out. Consequently, RCMs might be more sensitive to future changes in regional dynamics that could

lead to a reduction in vorticity. In contrast, GCMs may capture larger-scale atmospheric changes, such as shifts in jet stream patterns or baroclinicity, that RCMs might not fully capture. This divergence underscores the complexity of projecting future cyclone intensity and highlights the importance of considering both global and regional perspectives. However, both GCMs and RCMs agree that the most intense EETCs are likely to become more intense in the future, further amplifying their potential impacts. The projections for minimum MSLP are more consistent across models, showing a clear trend toward weaker cyclones. The combination of decreasing peak relative vorticity in RCMs and increasing minimum MSLP across models suggests that while intense cyclones might become less frequent, the spatial distribution and potential impacts of these storms could still be prominent, especially in regions where track density is projected to increase. The shift in spatial patterns, with fewer ETCs over the ocean and more over land, likely contributes to the projected reductions in cyclone duration, distance traveled, and intensity in future scenarios. This is consistent with the observation that ETCs over land tend to be shorter-lived and weaker than those over the ocean, which typically have access to greater moisture and energy, allowing them to sustain longer durations, travel greater distances, and exhibit higher intensities. The reduction in ETCs over the ocean in future scenarios may further amplify these trends, leading to weaker, shorter-lived cyclones overall.

The analysis of the METSSI reveals significant regional variations under future climate scenario. Specifically, we observed an increase in storm severity along the northern and southern coastal regions, particularly around Cape Town, while central and southeastern regions show a decrease. This suggests a potential shift in the distribution of extreme wind events, highlighting the need for targeted adaptation strategies in vulnerable coastal areas to mitigate the increased risks associated with future ETCs. Such strategies may include strengthening coastal infrastructure, updating building codes to withstand higher wind speeds, and enhancing early warning systems to improve preparedness. Additionally, these findings underscore the importance of integrating regional variations in storm severity into adaptation planning, ensuring that resources are allocated effectively to build resilience in areas most at risk.

A prominent reduction in ETC-associated rainfall over South Africa is observed in future projections, particularly in the southern regions around Cape Town (Reboita et al., 2021b). similarly project reduced ETC-associated rainfall across most of South Africa, with limited exceptions on the west coast. Yettella and Kay (2017) also noted a reduction in ETC-related precipitation over Africa, attributing it to weakened storm dynamics and reduced moisture availability. This reduction in ETC-related rainfall can be linked to several factors, including changes in atmospheric circulation patterns (Butler et al., 2010), a poleward shift in storm tracks (Bengtsson et al., 2006), and a decrease in the intensity of ETCs. These findings align with broader studies indicating a drying trend and increased drought frequency in the SH due to climate change. For instance, Engelbrecht et al. (2009) projected increased drought risk over southern Africa due to decreased winter rainfall, while Shongwe et al. (2009) reported a likely increase in the frequency of dry spells in the future. Similarly, studies by Christensen et al. (2007), and Schlosser et al. (2021) support these projections, indicating significant drying and more frequent drought conditions in southern Africa under future climate scenarios. Figure S16 in Supporting Information S1 in the appendix further illustrates the climatological seasonal average difference in precipitation for the winter season, showing a clear drying trend over South Africa in future projections. This trend underscores the critical need for adaptive measures to mitigate the adverse effects of reduced rainfall on water resources and agriculture in South Africa. While these findings indicate a decrease in ETC associated rainfall, it is essential to note that this does not necessarily imply a reduction in heavy rainfall events associated with ETCs. Pepler and Dowdy (2021, 2022) demonstrated that while total rainfall and the frequency of ETCs may decline in regions such as South Africa and Australia, the intensity of extreme rainfall events associated with ETCs is projected to remain steady or even increase under future climate scenarios. Their findings suggest that although total rainfall and storm frequency may decline, the intensity of extreme rainfall events could remain steady or even increase in some cases.

4. Conclusions

This study provides a comprehensive analysis of future changes in winter-time ETCs over South Africa using CORDEX-CORE simulations. The key findings indicate a consistent decrease in the frequency of ETCs across all GCM and RCM models under the RCP 8.5 scenario, suggesting a shift in mid-latitude weather patterns due to global warming. Projected changes reveal a shift in ETC track density, with decreases in southern and eastern parts of South Africa and increases along the west coast. The intensity of ETCs is generally projected to reduce in the future. However, both GCMs and RCMs consistently indicate that the most intense EETCs are projected to

become more intense, suggesting that these storms could lead to significant impacts, including stronger winds, heavier precipitation, and heightened risks to infrastructure and communities. METSSI shows notable regional variations, with increased storm severity in some areas despite the overall reduction in frequency, particularly along the northern and southern coastal regions. Additionally, there is a significant reduction in ETC-associated average rainfall over South Africa, especially in the southern regions around Cape Town, with notable increases in the South Indian Ocean, indicating a shift in the spatial distribution of rainfall. Additionally, the trends observed for EETCs are generally similar to those for regular ETCs, with a notable decrease in frequency but with regional variations in severity. These findings underscore the need for targeted adaptation strategies to mitigate the projected impacts of future ETCs on South Africa's climate and communities. Stakeholders must consider the reduction in frequency, changes in track density, variability in intensity, storm severity, and shifts in rainfall distribution to effectively address associated risks and challenges.

While our study provides valuable insights into the future behavior of ETCs over South Africa, it is important to acknowledge certain limitations and suggest areas for future research. The results are specific to our approach. Different approaches to cyclone tracking, defining cyclone intensity, and characterizing extremes might lead to variations in the projected impacts, highlighting the need for a multifaceted analytical approach. To improve the resolution of our projections, future studies could leverage higher-resolution model simulations, such as those provided by the Pan-African Convection-Permitting Regional Climate Simulation with the Met Office UM (CP4-Africa) model (Stratton et al., 2018) and HighResMIP Multimodel Ensembles (Roberts et al., 2020). These models offer finer spatial detail, which is crucial for accurately capturing localized climatic phenomena, particularly in regions with complex topography or along coastlines. One significant area for further exploration is the role of anti-cyclones, especially given the pronounced drying trends observed in our analysis. Investigating how changes in anti-cyclonic activity may influence regional climate patterns could provide a more complete understanding of future precipitation dynamics (A. Pepler, 2023; Reboita et al., 2019). Additionally, other types of cyclonic systems, such as cutoff lows (Muofhe et al., 2020; Pinheiro et al., 2019, 2021; Reboita et al., 2010; Xulu et al., 2023), which are known to have significant impacts on weather patterns over South Africa, could be examined to complement our findings on ETCs.

Data Availability Statement

CORDEX-CORE Africa (AFR-22) models and their driving GCM simulations were downloaded from https://esg-dn1.nsc.liu.se/search/cordex/ and can be accessed by searching for "CORDEX-CORE AFR-22" on the ESGF portal using parameters such as Project: CORDEX, Domain: AFR-22, relevant variables (e.g., temperature, precipitation), experiments (e.g., historical, rcp85), and the desired time period (e.g., 1950–2100). The objective feature tracking code developed by Kevin Hodges is available at https://doi.org/10.5281/zenodo.14441425 (K. Hodges, 2024). The ETC tracks and the processing codes are available at https://doi.org/10.5281/zenodo.14300915 (Chinta, 2024).

References

Abel, D., Ziegler, K., Gbode, I, E., Weber, T., Ajayi, V. O., et al. (2024). Robustness of climate indices relevant for agriculture in Africa deduced from GCMs and RCMs against reanalysis and gridded observations. *Climate Dynamics*, *62*(2), 1077–1106. https://doi.org/10.1007/s00382-023-06956-8

Bengtsson, L., Hagemann, S., & Hodges, K. I. (2004). Can climate trends be calculated from reanalysis data? *Journal of Geophysical Research D: Atmospheres*, *109*(11). https://doi.org/10.1029/2004JD004536

Bengtsson, L., Hodges, K. I., & Keenlyside, N. (2009). Will extratropical storms intensify in a warmer climate? *Journal of Climate*, *22*(9), 2276–2301. https://doi.org/10.1175/2008jcli2678.1

Bengtsson, L., Hodges, K. I., & Roeckner, E. (2006). Storm tracks and climate change. *Journal of Climate*, *19*(15), 3518–3543. https://doi.org/10.1175/JCLI3815.1

Bentsen, M., Bethke, I., Debernard, J. B., Iversen, T., Kirkevåg, A., Seland, Ø., et al. (2013). The Norwegian Earth System Model, NorESM1-M – Part 1: Description and basic evaluation of the physical climate. *Geoscientific Model Development*, *6*(3), 687–720. https://doi.org/10.5194/GMD-6-687-2013

Berry, G., Reeder, M. J., & Jakob, C. (2011). A global climatology of atmospheric fronts. *Geophysical Research Letters*, *38*(4). https://doi.org/10.1029/2010GL046451

Bodas-Salcedo, A., Hill, P. G., Furtado, K., Williams, K. D., Field, P. R., Manners, J. C., et al. (2016). Large contribution of supercooled liquid clouds to the solar radiation budget of the Southern Ocean. *Journal of Climate*, *29*(11), 4213–4228. https://doi.org/10.1175/JCLI-D-15-0564.1

Booth, J. F., Naud, C. M., & Willison, J. (2018). Evaluation of extratropical cyclone precipitation in the north Atlantic Basin: An analysis of ERA-Interim, WRF, and two CMIP5 models. *Journal of Climate*, *31*(6), 2345–2360. https://doi.org/10.1175/JCLI-D-17-0308.1

Butler, A. H., Thompson, D. W. J., & Heikes, R. (2010). The steady-state atmospheric circulation response to climate change–like thermal forcings in a simple general circulation model. *Journal of Climate*, *23*(13), 3474–3496. https://doi.org/10.1175/2010JCLI3228.1

Catto, J. L., Ackerley, D., Booth, J. F., Champion, A. J., Colle, B. A., Pfahl, S., et al. (2019). The future of midlatitude cyclones. *Current Climate Change Reports*, *5*(4), 407–420. https://doi.org/10.1007/s40641-019-00149-4

Catto, J. L., Jakob, C., Berry, G., & Nicholls, N. (2012). Relating global precipitation to atmospheric fronts. *Geophysical Research Letters*, *39*(10), 10805. https://doi.org/10.1029/2012GL051736

Catto, J. L., Shaffrey, L. C., & Hodges, K. I. (2010). Can climate models capture the structure of extratropical cyclones? *Journal of Climate*, *23*(7), 1621–1635. https://doi.org/10.1175/2009JCLI3318.1

Champion, A. J., Hodges, K. I., Bengtsson, L. O., Keenlyside, N. S., & Esch, M. (2011). Impact of increasing resolution and a warmer climate on extreme weather from Northern Hemisphere extratropical cyclones. *Tellus, Series A: Dynamic Meteorology and Oceanography*, *63*(5), 893–906. https://doi.org/10.1111/j.1600-0870.2011.00538.x

Chang, E. K. M. (2017). Projected significant increase in the number of extreme extratropical cyclones in the southern hemisphere. *Journal of Climate*, *30*(13), 4915–4935. https://doi.org/10.1175/JCLI-D-16-0553.1

Chang, E. K. M., Guo, Y., & Xia, X. (2012). CMIP5 multimodel ensemble projection of storm track change under global warming. *Journal of Geophysical Research*, *117*(D23), D23118. https://doi.org/10.1029/2012JD018578

Chang, E. K. M., Guo, Y., Xia, X., & Zheng, M. (2013). Storm-track activity in IPCC AR4/CMIP3 model simulations. *Journal of Climate*, *26*(1), 246–260. https://doi.org/10.1175/JCLI-D-11-00707.1

Chinta, S. (2024). Data and processing codes for "future changes in winter-time extratropical cyclones over South Africa from CORDEX-CORE simulations [Dataset/Code]. *Zenodo*. https://doi.org/10.5281/zenodo.14300915

Christensen, J. H., Hewitson, B., Busuioc, A., Chen, A., Gao, X., Held, I., et al. (2007). Regional climate projections. In *Climate change 2007: The physical science basis. Contribution of working group I to the fourth assessment report of the intergovernmental panel on climate change*. Cambridge University Press.

Christensen, J. H., Krishna Kumar, K., Aldrian, E., An, S.-I., Cavalcanti, I. F. A., de Castro, M. J. A., et al. (2013). Climate phenomena and their relevance for future regional climate change. *Climate Change 2013: The Physical Science Basis. Contribution of Working Group I to the Fifth Assessment Report of the Intergovernmental Panel on Climate Change*. https://doi.org/10.1017/CBO9781107415324.028

Conradie, W. S., Wolski, P., & Hewitson, B. C. (2022). Spatial heterogeneity in rain-bearing winds, seasonality and rainfall variability in southern Africa's winter rainfall zone. *Advances in Statistical Climatology, Meteorology and Oceanography*, *8*(1), 31–62. https://doi.org/10.5194/ascmo-8-31-2022

Coppola, E., Raffaele, F., Giorgi, F., Giuliani, G., Xuejie, G., Ciarlo, J. M., et al. (2021). Climate hazard indices projections based on CORDEX-CORE, CMIP5 and CMIP6 ensemble. *Climate Dynamics*, *57*(5–6), 1293–1383. https://doi.org/10.1007/S00382-021-05640-Z/FIGURES/13

Dee, D. P., Uppala, S. M., Simmons, A. J., Berrisford, P., Poli, P., Kobayashi, S., et al. (2011). The ERA-interim reanalysis: Configuration and performance of the data assimilation system. *Quarterly Journal of the Royal Meteorological Society*, *137*(656), 553–597. https://doi.org/10.1002/QJ.828

Denis, B., Côté, J., & Laprise, R. (2002). Spectral decomposition of two-dimensional atmospheric fields on limited-area domains using the Discrete Cosine Transform (DCT). *Monthly Weather Review*, *130*(7), 1812–1829. https://doi.org/10.1175/1520-0493(2002)130

Dowdy, A. J., Mills, G. A., Timbal, B., & Wang, Y. (2013). Changes in the risk of extratropical cyclones in Eastern Australia. *Journal of Climate*, *26*(4), 1403–1417. https://doi.org/10.1175/JCLI-D-12-00192.1

Elguindi, N., Giorgi, F., & Turuncoglu, U. (2014). Assessment of CMIP5 global model simulations over the subset of CORDEX domains used in the Phase I CREMA. *Climatic Change*, *125*(1), 7–21. https://doi.org/10.1007/S10584-013-0935-9/FIGURES/4

Engelbrecht, F. A., McGregor, J. L., & Engelbrecht, C. J. (2009). Dynamics of the conformal-cubic atmospheric model projected climate-change signal over southern Africa. *International Journal of Climatology*, *29*(7), 1013–1033. https://doi.org/10.1002/JOC.1742

Fasullo, J. T., & Trenberth, K. E. (2008). The annual cycle of the energy budget. Part II: Meridional structures and poleward transports. *Journal of Climate*, *21*(10), 2313–2325. https://doi.org/10.1175/2007JCLI1936.1

Forzieri, G., Feyen, L., Russo, S., Vousdoukas, M., Alfieri, L., Outten, S., et al. (2016). Multi-hazard assessment in Europe under climate change. *Climatic Change*, *137*(1–2), 105–119. https://doi.org/10.1007/s10584-016-1661-x

Geng, Q., & Sugi, M. (2003). Possible change of extratropical cyclone activity due to enhanced greenhouse gases and sulfate aerosols – Study with a high-resolution AGCM. *Journal of Climate*, *16*(13), 2262–2274. https://doi.org/10.1175/1520-0442(2003)16<2262:PCOECA>2.0.CO;2

Giorgetta, M. A., Jungclaus, J., Reick, C. H., Legutke, S., Bader, J., Böttinger, M., et al. (2013). Climate and carbon cycle changes from 1850 to 2100 in MPI-ESM simulations for the Coupled Model Intercomparison Project phase 5. *Journal of Advances in Modeling Earth Systems*, *5*(3), 572–597. https://doi.org/10.1002/JAME.20038

Giorgi, F. (2019). Thirty years of regional climate modeling. Where are we and where are we going next? *Journal of Geophysical Research: Atmospheres*, *124*(11), 5606–5723. https://doi.org/10.1029/2018JD030094

Giorgi, F., Coppola, E., Solmon, F., Mariotti, L., Sylla, M. B., Bi, X., et al. (2012). RegCM4: Model description and preliminary tests over multiple CORDEX domains. *Climate Research*, *52*(1), 7–29. https://doi.org/10.3354/CR01018

Giorgi, F., Coppola, E., Teichmann, C., & Jacob, D. (2021). Editorial for the CORDEX-CORE experiment I special issue 1 the CORDEX-CORE initiative. *Climate Dynamics*, *57*(5–6), 1265–1268. https://doi.org/10.1007/s00382-021-05902-w

Giorgi, F., Jones, C., & Asrar, G. R. (2009). Addressing climate information needs at the regional level: The CORDEX framework. *World Meteorological Organization Bulletin*, *58*(3), 175–183.

Gutowski, W. J., Giorgi, F., Timbal, B., Frigon, A., Jacob, D., Kang, H. S., et al. (2016). WCRP COordinated regional downscaling EXperiment (CORDEX): A diagnostic MIP for CMIP6. *Geoscientific Model Development*, *9*(11), 4087–4095. https://doi.org/10.5194/gmd-9-4087-2016

Hawcroft, M., Walsh, E., Hodges, K., & Zappa, G. (2018). Significantly increased extreme precipitation expected in Europe and North America from extratropical cyclones. *Environmental Research Letters*, *13*(12), 124006. https://doi.org/10.1088/1748-9326/AAED59

Hawcroft, M. K., Shaffrey, L. C., Hodges, K. I., & Dacre, H. F. (2012). How much Northern Hemisphere precipitation is associated with extratropical cyclones? *Geophysical Research Letters*, *39*(24). https://doi.org/10.1029/2012GL053866

Held, I. M., & Soden, B. J. (2006). Robust responses of the hydrological cycle to global warming. *Journal of Climate*, *19*(21), 5686–5699. https://doi.org/10.1175/JCLI3990.1

Hodges, K. (2024). Track [Software]. *Zenodo*. https://doi.org/10.5281/zenodo.14441425

Hodges, K. I. (1994). A general method for tracking analysis and its application to meteorological data. *Monthly Weather Review*, *122*(11), 2573–2586. https://doi.org/10.1175/1520-0493(1994)122<2573:agmfta>2.0.co;2

Hodges, K. I. (1995). Feature tracking on the unit sphere. *Monthly Weather Review*, *123*(12), 3458–3465. https://doi.org/10.1175/1520-0493(1995)123<3458:ftotus>2.0.co;2

Hodges, K. I. (1999). Adaptive constraints for feature tracking. *Monthly Weather Review*, *127*(6), 1362–1373. https://doi.org/10.1175/1520-0493(1999)127<1362:acfft>2.0.co;2

Hodges, K. I., Lee, R. W., & Bengtsson, L. (2011). A comparison of extratropical cyclones in recent reanalyses ERA-Interim, NASA MERRA, NCEP CFSR, and JRA-25. *Journal of Climate*, *24*(18), 4888–4906. https://doi.org/10.1175/2011JCLI4097.1

Hoskins, B. J., & Hodges, K. I. (2002). New perspectives on the Northern Hemisphere winter storm tracks. *Journal of the Atmospheric Sciences*, *59*(6), 1041–1061. https://doi.org/10.1175/1520-0469(2002)059<1041:npotnh>2.0.co;2

Iles, C. E., Vautard, R., Strachan, J., Joussaume, S., Eggen, B. R., & Hewitt, C. D. (2020). The benefits of increasing resolution in global and regional climate simulations for European climate extremes. *Geoscientific Model Development*, *13*(11), 5583–5607. https://doi.org/10.5194/GMD-13-5583-2020

Iversen, T., Bentsen, M., Bethke, I., Debernard, J. B., Kirkevåg, A., Seland, Ø., et al. (2013). The Norwegian Earth System Model, NorESM1-M – Part 2: Climate response and scenario projections. *Geoscientific Model Development*, *6*(2), 389–415. https://doi.org/10.5194/GMD-6-389-2013

Jacob, D., Elizalde, A., Haensler, A., Hagemann, S., Kumar, P., Podzun, R., et al. (2012). Assessing the transferability of the regional climate model REMO to different COordinated regional climate downscaling EXperiment (CORDEX) regions. *Atmosphere*, *3*(1), 181–199. https://doi.org/10.3390/ATMOS3010181

Jacob, D., Teichmann, C., Sobolowski, S., Katragkou, E., Anders, I., Belda, M., et al. (2020). Regional climate downscaling over Europe: Perspectives from the EURO-CORDEX community. *Regional Environmental Change*, *20*(2), 51. https://doi.org/10.1007/s10113-020-01606-9

Karremann, M. K. (2015). *Return periods and clustering of potential losses associated with European windstorms in a changing climate: PhD thesis*. Universität zu Köln.

Karremann, M. K., Pinto, J. G., Reyers, M., & Klawa, M. (2014). Return periods of losses associated with European windstorm series in a changing climate. *Environmental Research Letters*, *9*(12), 124016. https://doi.org/10.1088/1748-9326/9/12/124016

Karremann, M. K., Pinto, J. G., Von Bomhard, P. J., & Klawa, M. (2014). On the clustering of winter storm loss events over Germany. *Natural Hazards and Earth System Sciences*, *14*(8), 2041–2052. https://doi.org/10.5194/nhess-14-2041-2014

Klawa, M., & Ulbrich, U. (2003). A model for the estimation of storm losses and the identification of severe winter storms in Germany. *Natural Hazards and Earth System Sciences*, *3*(6), 725–732.

Leckebusch, G. C., Ulbrich, U., Fröhlich, L., & Pinto, J. G. (2007). Property loss potentials for European midlatitude storms in a changing climate. *Geophysical Research Letters*, *34*(5). https://doi.org/10.1029/2006GL027663

Lehmann, J., Coumou, D., Frieler, K., Eliseev, A. V., & Levermann, A. (2014). Future changes in extratropical storm tracks and baroclinicity under climate change. *Environmental Research Letters*, *9*(8), 84002. https://doi.org/10.1088/1748-9326/9/8/084002

Lennard, C. J., Coop, L., Morison, D., & Grandin, R. (2013). Extreme events: Past and future changes in the attributes of extreme rainfall and the dynamics of their driving processes Report to the Water Research Commission. www.wrc.org.za

Lionello, P., Dalan, F., & Elvini, E. (2002). Cyclones in the Mediterranean region: The present and the doubled CO2 climate scenarios. *Climate Research*, *22*(2), 147–159. https://doi.org/10.3354/CR022147

Little, A. S., Priestley, M. D. K., & Catto, J. L. (2023). Future increased risk from extratropical windstorms in northern Europe. *Nature Communications*, *14*(1), 4434. https://doi.org/10.1038/s41467-023-40102-6

MacKellar, N. C., Hewitson, B. C., & Tadross, M. A. (2007). Namaqualand's climate: Recent historical changes and future scenarios. *Journal of Arid Environments*, *70*(4), 604–614. https://doi.org/10.1016/J.JARIDENV.2006.03.024

Mahlobo, D., Engelbrecht, F., Ndarana, T., Abubakar, H. B., Olabanji, M. F., & Ncongwane, K. (2024). Analysis of the Hadley cell, subtropical anticyclones and their effect on South African rainfall. *Theoretical and Applied Climatology*, *155*(2), 1035–1054. https://doi.org/10.1007/s00704-023-04674-z

McErlich, C., McDonald, A., Schuddeboom, A., Vishwanathan, G., Renwick, J., & Rana, S. (2023). Positive correlation between wet-day frequency and intensity linked to universal precipitation drivers. *Nature Geoscience*, *16*(5), 410–415. https://doi.org/10.1038/s41561-023-01177-4

Mearns, L. O., Giorgi, F., McDaniel, L., & Shields, C. (2012). Analysis of climate variability and diurnal temperature range from the NARCCAP regional climate model simulations. *Journal of Geophysical Research*, *117*(D3).

Mizuta, R., Matsueda, M., Endo, H., & Yukimoto, S. (2011). Future change in extratropical cyclones associated with change in the upper troposphere. *Journal of Climate*, *24*(24), 6456–6470. https://doi.org/10.1175/2011JCLI3969.1

Moon, W., Kim, B. M., Yang, G. H., & Wettlaufer, J. S. (2022). Wavier jet streams driven by zonally asymmetric surface thermal forcing. *Proceedings of the National Academy of Sciences of the United States of America*, *119*(38). https://doi.org/10.1073/PNAS.2200890119/FORMAT/EPUB

Muofhe, T. P., Chikoore, H., Bopape, M. J. M., Nethengwe, N. S., Ndarana, T., & Rambuwani, G. T. (2020). Forecasting intense cut-off lows in South Africa using the 4.4 km unified model. *Climate*, *8*(11), 1–20. https://doi.org/10.3390/cli8110129

Murakami, H., Mizuta, R., & Shindo, E. (2012). Future changes in tropical cyclone activity projected by multi-physics and multi-SST ensemble experiments using the 60-km-mesh MRI AGCM. *Climate Dynamics*, *39*(9–10), 2569–2584. https://doi.org/10.1007/s00382-011-1223-x

Palipane, E., Lu, J., Staten, P., Chen, G., & Schneider, E. K. (2017). Investigating the zonal wind response to SST warming using transient ensemble AGCM experiments. *Climate Dynamics*, *48*(1–2), 523–540. https://doi.org/10.1007/S00382-016-3092-9/FIGURES/14

Parsons, S., Renwicka, J. A., & McDonald, A. J. (2016). An assessment of future southern hemisphere blocking using CMIP5 projections from four GCMs. *Journal of Climate*, *29*(21), 7599–7611. https://doi.org/10.1175/JCLI-D-15-0754.1

Peixoto, J. P., & Oort, A. H. (1992). *Physics of climate*. American Institute of Physics. Retrieved from https://www.osti.gov/biblio/7287064

Pepler, A. (2023). Projections of synoptic anticyclones for the twenty-first century. *Climate Dynamics*, *61*(7–8), 3271–3287. https://doi.org/10.1007/S00382-023-06728-4/FIGURES/10

Pepler, A., & Dowdy, A. (2021). Fewer deep cyclones projected for the midlatitudes in a warming climate, but with more intense rainfall. *Environmental Research Letters*, *16*(5), 054044. https://doi.org/10.1088/1748-9326/ABF528

Pepler, A. S., & Dowdy, A. J. (2022). Australia's future extratropical cyclones. *Journal of Climate*, *35*(23), 7795–7810. https://doi.org/10.1175/JCLI-D-22-0312.1

Pfahl, S., & Wernli, H. (2012). Quantifying the relevance of cyclones for precipitation extremes. *Journal of Climate*, *25*(19), 6770–6780. https://doi.org/10.1175/JCLI-D-11-00705.1

Pinheiro, H., Gan, M., & Hodges, K. (2021). Structure and evolution of intense austral cut-off lows. *Quarterly Journal of the Royal Meteorological Society*, *147*(734), 1–20. https://doi.org/10.1002/qj.3900

Pinheiro, H. R., Hodges, K. I., & Gan, M. A. (2019). Sensitivity of identifying cut-off lows in the Southern Hemisphere using multiple criteria: Implications for numbers, seasonality and intensity. *Climate Dynamics*, *53*(11), 6699–6713. https://doi.org/10.1007/s00382-019-04984-x

Pinto, J. G., Fröhlich, E. L., Leckebusch, G. C., & Ulbrich, U. (2007). Changing European storm loss potentials under modified climate conditions according to ensemble simulations of the ECHAM5/MPI-OM1 GCM. *Natural Hazards and Earth System Sciences*, *7*(1), 165–175. https://doi.org/10.5194/NHESS-7-165-2007

Pinto, J. G., Karremann, M. K., Born, K., Della-Marta, P. M., & Klawa, M. (2012). Loss potentials associated with European windstorms under future climate conditions. *Climate Research*, *54*(1), 1–20. https://doi.org/10.3354/CR01111

Priestley, M. D. K., & Catto, J. L. (2022a). Future changes in the extratropical storm tracks and cyclone intensity, wind speed, and structure. *Weather and Climate Dynamics*, *3*(1), 337–360. https://doi.org/10.5194/wcd-3-337-2022

Priestley, M. D. K., & Catto, J. L. (2022b). Improved representation of extratropical cyclone structure in HighResMIP models. *Geophysical Research Letters*, *49*(5). https://doi.org/10.1029/2021GL096708

Reale, M., & Lionello, P. (2013). Synoptic climatology of winter intense precipitation events along the Mediterranean coasts. *Natural Hazards and Earth System Sciences*, *13*(7), 1707–1722. https://doi.org/10.5194/NHESS-13-1707-2013

Reboita, M. S., Ambrizzi, T., Silva, B. A., Pinheiro, R. F., & da Rocha, R. P. (2019). The south atlantic subtropical anticyclone: Present and future climate. *Frontiers in Earth Science*, *7*, 430450. https://doi.org/10.3389/FEART.2019.00008/BIBTEX

Reboita, M. S., Crespo, N. M., Torres, J. A., Reale, M., da Rocha, R. P., Giorgi, F., & Coppola, E. (2021). Future changes in winter explosive cyclones over the Southern Hemisphere domains from the CORDEX-CORE ensemble. *Climate Dynamics*, *57*(11–12), 3303–3322. https://doi.org/10.1007/s00382-021-05867-w

Reboita, M. S., da Rocha, R. P., de Souza, M. R., & Llopart, M. (2018). Extratropical cyclones over the southwestern South Atlantic Ocean: HadGEM2-ES and RegCM4 projections. *International Journal of Climatology*, *38*(6), 2866–2879. https://doi.org/10.1002/joc.5468

Reboita, M. S., Nieto, R., Gimeno, L., Da Rocha, R. P., Ambrizzi, T., Garreaud, R., & Krger, L. F. (2010). Climatological features of cutoff low systems in the Southern Hemisphere. *Journal of Geophysical Research*, *115*(17). https://doi.org/10.1029/2009JD013251

Reboita, M. S., Reale, M., da Rocha, R. P., Giorgi, F., Giuliani, G., Coppola, E., et al. (2021). Future changes in the wintertime cyclonic activity over the CORDEX-CORE southern hemisphere domains in a multi-model approach. *Climate Dynamics*, *57*, 1533–1549. https://doi.org/10.1007/s00382-020-05317-z

Remedio, A. R., Teichmann, C., Buntemeyer, L., Sieck, K., Weber, T., Rechid, D., et al. (2019). Evaluation of new CORDEX simulations using an updated Köppen–Trewartha climate classification. *Atmosphere*, *10*(11), 726. https://doi.org/10.3390/ATMOS10110726

Roberts, J. F., Champion, A. J., Dawkins, L. C., Hodges, K. I., Shaffrey, L. C., Stephenson, D. B., et al. (2014). The XWS open access catalogue of extreme European windstorms from 1979 to 2012. *Natural Hazards and Earth System Sciences*, *14*(9), 2487–2501. https://doi.org/10.5194/nhess-14-2487-2014

Roberts, M. J., Camp, J., Seddon, J., Vidale, P. L., Hodges, K., Vannière, B., et al. (2020). Projected future changes in tropical cyclones using the CMIP6 HighResMIP multimodel ensemble. *Geophysical Research Letters*, *47*(14), e2020GL088662. https://doi.org/10.1029/2020GL088662

Safari, B., Sebaziga, J. N., & Siebert, A. (2023). Evaluation of CORDEX-CORE regional climate models in simulating rainfall variability in Rwanda. *International Journal of Climatology*, *43*(2), 1112–1140. https://doi.org/10.1002/joc.7891

Schlosser, A., Sokolov, A., Strzepek, K., Thomas, T., Gao, X., Arndt, C., & Arndt, C. (2021). The changing nature of hydroclimatic risks across South Africa. *Climatic Change*, *168*(3–4), 28. https://doi.org/10.1007/s10584-021-03235-5

Shongwe, M. E., Van Oldenborgh, G. J., Van Den Hurk, B. J. J. M., De Boer, B., Coelho, C. A. S., & Van Aalst, M. K. (2009). Projected changes in mean and extreme precipitation in Africa under global warming. Part I: Southern Africa. *Journal of Climate*, *22*(13), 3819–3837. https://doi.org/10.1175/2009JCLI2317.1

Sinclair, V. A., & Catto, J. L. (2023). The relationship between extra-tropical cyclone intensity and precipitation in idealised current and future climates. *Weather and Climate Dynamics*, *4*(3), 567–589. https://doi.org/10.5194/wcd-4-567-2023

Sinclair, V. A., Rantanen, M., Haapanala, P., Räisänen, J., & Järvinen, H. (2020). The characteristics and structure of extra-tropical cyclones in a warmer climate. *Weather and Climate Dynamics*, *1*, 1–25. https://doi.org/10.5194/wcd-1-1-2020

Sørland, S. L., Brogli, R., Pothapakula, P. K., Russo, E., Van De Walle, J., Ahrens, B., et al. (2021). COSMO-CLM regional climate simulations in the Coordinated Regional Climate Downscaling Experiment (CORDEX) framework: A review. *Geoscientific Model Development*, *14*(8), 5125–5154. https://doi.org/10.5194/GMD-14-5125-2021

Stevens, B., Giorgetta, M., Esch, M., Mauritsen, T., Crueger, T., Rast, S., et al. (2013). Atmospheric component of the MPI-M Earth System Model: ECHAM6. *Journal of Advances in Modeling Earth Systems*, *5*(2), 146–172. https://doi.org/10.1002/JAME.20015

Stratton, R. A., Senior, C. A., Vosper, S. B., Folwell, S. S., Boutle, I. A., Earnshaw, P. D., et al. (2018). A Pan-African convection-permitting regional climate simulation with the Met Office unified model: CP4-Africa. *Journal of Climate*, *31*(9), 3485–3508. https://doi.org/10.1175/JCLI-D-17-0503.1

Tamarin, T., & Kaspi, Y. (2016). The poleward motion of extratropical cyclones from a potential vorticity tendency analysis. *Journal of the Atmospheric Sciences*, *73*(4), 1687–1707. https://doi.org/10.1175/JAS-D-15-0168.1

Torres-Alavez, J. A., Glazer, R., Giorgi, F., Coppola, E., Gao, X., Hodges, K. I., et al. (2021). Future projections in tropical cyclone activity over multiple CORDEX domains from RegCM4 CORDEX-CORE simulations. *Climate Dynamics*, *57*(5–6), 1507–1531. https://doi.org/10.1007/s00382-021-05728-6

Trenberth, K. E., & Stepaniak, D. P. (2004). The flow of energy through the earth's climate system. *Part B No. 603 Q. J. R. Meteorol. Soc*, *130*, 2677–2701. https://doi.org/10.1256/qj.04.83

Ulbrich, U., Leckebusch, G. C., & Pinto, J. G. (2009). Extra-tropical cyclones in the present and future climate: A review. *Theoretical and Applied Climatology*, *96*(1–2), 117–131. https://doi.org/10.1007/S00704-008-0083-8/FIGURES/2

Utsumi, N., Kim, H., Kanae, S., & Oki, T. (2017). Relative contributions of weather systems to mean and extreme global precipitation. *Journal of Geophysical Research: Atmospheres*, *122*(1), 152–167. https://doi.org/10.1002/2016JD025222

Xulu, N. G., Chikoore, H., Bopape, M. J. M., Ndarana, T., Muofhe, T. P., Mbokodo, I. L., et al. (2023). Cut-off lows over South Africa: A review. In *Climate* (Vol. 11(3), p. 59). MDPI. https://doi.org/10.3390/cli11030059

Yettella, V., & Kay, J. E. (2017). How will precipitation change in extratropical cyclones as the planet warms? Insights from a large initial condition climate model ensemble. *Climate Dynamics*, *49*(5–6), 1765–1781. https://doi.org/10.1007/s00382-016-3410-2

Zappa, G., Shaffrey, L. C., & Hodges, K. I. (2013). The ability of CMIP5 models to simulate north Atlantic extratropical cyclones. *Journal of Climate*, *26*(15), 5379–5396. https://doi.org/10.1175/JCLI-D-12-00501.1